Orientation-dependent epitaxial growth of GaAs by current-controlled liquid phase epitaxy

メタデータ	言語: eng
	出版者:
	公開日: 2011-05-22
	キーワード (Ja):
	キーワード (En):
	作成者: Mouleeswaran, D., Koyama, T., Hayakawa, Yasuhiro
	メールアドレス:
	所属:
URL	http://hdl.handle.net/10297/5644

Orientation-dependent epitaxial growth of GaAs by current-controlled liquid phase epitaxy

D. Mouleeswaran, T. Koyama and Y. Hayakawa*

Research Institute of Electronics, Shizuoka University, 3-5-1 Johoku, Naka-ku, Hamamatsu,

Shizuoka 432-8011, Japan

Abstract

The orientation dependence of the selective epitaxial growth of Gallium Arsenide (GaAs) has been investigated to achieve a thick epitaxial layer for application to X-ray detectors. Selective epitaxial growth was carried out on patterned GaAs with [011], [012], [010], [01-2], [01-1] and their equivalent seed orientations by current controlled liquid phase epitaxy (CCLPE). SiO_2 was used as a mask layer to fabricate the various seed orientations on the Si-doped GaAs (100) substrate and various growth periods and current densities were considered. Solute transport in the solution was enhanced by the electromigration of solute by an applied DC electric current, which caused an incremental growth in vertical and lateral directions in all orientations. The highest vertical thickness of 268 μm in the [01-1] orientation and the largest lateral growth of 318 μm in the [012] orientation were achieved at 7.5 Acm^{-2} current density for 6 h. The seed aligned in the [012] orientation was favorable for high lateral growth of GaAs. The [011], [010] and [01-2] seed orientations were suitable for application in a GaAs X-ray detector.

∗*Corresponding author:*

Yasuhiro Hayakawa
Research Institute of Electronics,
Shizuoka University,
3-5-1, Johoku, Naka-ku,Hamamatsu 432-8011, Japan.
TEL/FAX: 053-478-1310.
E-mail: royhaya@ipc.shizuoka.ac.jp

1. Introduction

Digital imaging technology has opened a new horizon to the development of X-ray medical imaging detectors [1]. Since multiple exposure to radiation creates permanent cell damage in a patient's body, X-ray medical imaging detectors with high detection efficiency are required. Commercial X-ray medical imaging detectors are either scintillator material coupled to an array of silicon-based flat panel photo detectors called indirect conversion detectors or amorphous-selenium (a-selenium)-based detectors called direct conversion detectors. In indirect conversion detectors, the scintillator absorbs X-rays and generates light. The light is then detected by an array of photodetectors. The silicon-based photodetectors are widely used in medical imaging systems. Silicon material technology has established itself over the past two decades, although silicon has a drawback, an indirect bandgap which restricts the detection efficiency and device performance. In direct conversion within a-selenium-based detectors, the X-ray is absorbed and electrical signals are created in one step. The active material is in an amorphous nature which limits the number of e-h pairs generated due to many discrete defect levels [2-4]. Single crystalline material of commercial detectors has been replaced by direct bandgap material, which improves the detection efficiency and device performance considerably by direct conversion of photons to electrons. A 1.5 eV bandgap is enough to overcome the electronic noise and to produce a maximum number of e-h pairs at room temperature.

Recently, Gallium Arsenide (GaAs) has received much attention in X-ray medical imaging detector application ranging from 5-30 keV. It has a direct bandgap of 1.42 eV and shows a good X-ray absorption coefficient compared to Cadmium Telluride (CdTe) [5,6]. Both GaAs and CdTe have equivalent mobility life times ($\mu\tau$). The higher mobility (μ) in GaAs is compensated by a slightly longer life time (τ) value in CdTe. However, GaAs has some

advantages compared to CdTe such as large dimension growth, device integration with existing monolithic technology, and it is cost effective. The next generation of X-ray medical imaging devices will be based on GaAs detectors.

GaAs crystal growth technology is well established and one can obtain 6-inch wafers commercially by either liquid-encapsulated Czochralski (LEC) or vertical gradient freezing (VGF) growth methods. The crystal contains a large concentration of defects due to a growth temperature close to the melting point of GaAs and is consequently characterized by a rather high concentration of deep traps related to native defects which are distributed non-uniformly along its orientations. In X-ray detector applications, the charge collection efficiency depends on these defect concentrations and is decreased by non-radiative recombination. The currently available quality of wafers is still lacking for efficient X-ray imaging detector fabrication. For application to X-ray detectors, the depletion layer of the device should be thick enough to withstand high potential to collect the charge carriers generated by the radiation. Therefore, a thick epilayer of dislocation-free GaAs of more than 100 μm is essential for X-ray imaging devices.

GaAs epitaxial layers have been grown by many methods such as liquid phase epitaxy (LPE), liquid phase electro epitaxy (LPEE), the temperature difference method (TDM) and many kinds of vapor phase epitaxy (VPE). Some studies have been devoted to growing a thick GaAs epilayer by hydride-vapor phase epitaxy (HVPE) [10,11]. However, VPE has certain limitations to achieve a thick layer since a long growth period is required or a huge amount of gas is consumed. A thick epilayer can be grown by LPE, LPEE and TDM. However, the dislocation density of the epilayers is still high. Selective epitaxial growth technology is a viable method to prevent the propagation of defects from the substrate to the epitaxial layer [15-27]. However,

investigation on the selective epitaxial growth of GaAs is concentrated only on lateral growth rather than on the thick epilayer.

Nishinaga et al investigated the growth of an GaAs epilayer on GaAs (111)B star patterned substrate by LPE and Si (111) substrate by combination of molecular beam epitaxy (MBE) and LPE [28-30]. The width of the line seed used for these investigations was less than 5 µm. The orientation of the line seed opening was rotated every ±15°. The investigation was mainly devoted to understanding the dependence of epitaxial lateral growth on various seed directions and showed that the ELO layer grown on the seed tilted away from the [100], [110], [010], [-110] and their equivalent orientations was wide and flat. In contrast to their work, the present investigation aims to investigate the orientation-dependent selective growth of GaAs by current and to identify the suitable orientation for thick GaAs epilayer growth for X-ray detector application. To grow a thick epilayer, a combination of standard LPE method with a flow of DC electric current, termed current-controlled liquid phase epitaxy (CCLPE), was used. In CCLPE, Peltier cooling at the solution-substrate interface, diffusion and electromigration contributes to overall epitaxial growth. To the best of our knowledge, no detailed investigations on orientation-dependent GaAs epilayer growth by CCLPE have been reported. An epilayer thickness of more than 200 µm is achieved within a relatively reduced growth period of 6 h by a flowing DC electric current of 7.5 Acm^{-2} in CCLPE.

2. Experimental details

SiO$_2$ was used as a mask layer to fabricate various seed orientations on Si-doped GaAs (100) substrate by standard photolithography and a wet chemical etching method. Prior to SiO$_2$ mask deposition, the substrate was washed with de-ionized water, acetone and ethanol in

ultrasonic cleaning to remove organic contaminants on the substrate; subsequently, to remove native oxides by H_2SO_4:H_2O_2:H_2O in a ratio of 3:1:1, the substrate was ultrasonicated for 30 sec at 65°C. The OCD chemical solution was used as a source material for SiO_2 and it was deposited on the substrate by spin coating followed by annealing at 600°C for 30 min in an argon atmosphere for good bonding with the substrate. The thickness of the mask layer was about 0.2 μm. The star seed pattern was formed on the SiO_2 mask by standard photolithography. The seed windows were opened by BHF etching for 5 sec. A schematic diagram of the substrate with seed orientations is shown in Fig. 1. The orientation of the seed windows was [011], [012], [010] and their equivalent directions. The width of the seed window was 500 μm and the angle between the seed windows was ± 22.5°.

The system used for this investigation was a standard LPE system, which had been modified to flow an electric current during growth. The substrate was loaded into the system together with 3 g gallium, polycrystalline GaAs and 10^{-4} atomic concentration of Te as a dopant. The design of the CCLPE growth bin and system construction is described in another paper [31]. Baking of the source material was carried out to ensure solubility of GaAs in gallium solution. The growth solution was kept at 850°C for 4 h to homogeneously mix gallium and GaAs. The temperature of the solution was cooled down to a growth temperature of 800°C at a cooling rate of 0.8°C/min. At 800°C, the solution was placed into contact with dummy substrate for 1 h to ensure a saturated solution for growth, termed stabilization. After stabilization, the solution was removed from the dummy substrate and subsequently the furnace temperature was cooled at a rate of 0.6°C /min. When the solution temperature reached 797°C, the substrate made contact with solution, and subsequently a current was applied to the solution through the substrate. Growth was terminated by cutting off the current and removing the solution from the substrate.

The investigation was carried out with and without a current to analyze the epitaxial growth of GaAs at different orientations. The direction of the current is always from the substrate to the solution. The current density (J) is defined by the applied current divided by the contact area on the substrate. The growth period (0.5-6 h) and applied current density (0-7.5 Acm^{-2}) were varied to investigate the selective epitaxial growth process of CCLPE. The morphology of selectively grown epilayers was analyzed using a scanning electron microscope (SEM) and etch pit density (EPD) was analyzed along a laterally grown epilayer in the [012] orientation by molten KOH etching for 2 min.

3. Results and discussion

3.1 Star pattern growth by LPE

The GaAs epilayer was grown on the star patterned GaAs (100) substrate by LPE for 0.5 h to 6 h. The right hand quarter of the grown GaAs epilayer was considered for discussion because the remainder of all its equivalent orientations showed similar growth characteristics. Fig. 2(a)-(d) shows a bird's eye view of selective epitaxial growth of the GaAs epilayer on seed orientations [011], [012], [010], [01-2], and [01-1] at (a) 0.5 h, (b) 2 h, (c) 3 h, and (d) 6 h, respectively. Initially, epitaxial growth was restricted only in the window region and the GaAs layer was grown slightly in a lateral direction after 0.5 h growth. After a growth period of 2 h, considerable lateral growth was observed in all orientations. A zigzag step growth pattern was formed along the laterally grown epilayer. The surface of the epilayers grown at the seed window in the [011], [01-1] orientation was comparatively smooth, whereas surface roughness was higher in [012], [010] and [01-2] orientations. When the growth period was increased to 3 h, the surface roughness of the epilayers grown along [011], [012] and [010] orientations was higher

compared to [01-2], [01-1] orientations. After 6 h growth, the smooth epilayers had grown in all orientations except for the [011] orientation which has some voids on the surface. In the [012] orientation, the {111} facet was formed at the front top, which was identified by the angle of deviation from the substrate plane. The {111} facet restricts further lateral growth due to its low surface energy. The width of lateral growth increased with the distance from the origin of the [012] orientation. Since the cooling rate is fixed, the supply of solutes due to diffusion from solution to the seed window was constant at all orientations. However, high lateral growth was observed in the [012] orientation compared to other orientations. The side face of the [012] orientation was identified as 1.6° off orientated {112} planes. Since the higher order plane has larger steps, it is easy to grow by attracting more solute atoms to the side faces from the top (100) face. On the other hand, vertical growth is limited by the formation of the {100} facet on the top. In the [010] orientation, sluggish lateral growth was observed compared to the [012] orientation. The side faces are {110} planes, which are identified by a 45° angle between the side plane and the substrate plane. Since {110} planes have a small number of steps, lateral growth is suppressed. The canal-like epilayer structure is grown along the [01-2] orientation. The side faces are identified as 1.5° off the orientated {311} plane. As this plane has a large number of steps, lateral growth is enhanced. In the [01-1] orientation, the epilayer is grown in the seed window with a smooth surface.

The epitaxial growth can be explained with respect to time as follows: Consider epitaxial growth in the [010] orientation with respect to time. Initially no macro steps are observed in the seed window. After 2 h growth, the steps with a crest and trough structure are partially formed in the seed window and are connected the window wall through its step-crest. When growth proceeds up to 3 h, the window walls are completely connected by the step crest. The step-

troughs look like a void in the seed window. When the growth period is further increased to 6 h, the step troughs are filled by epitaxial growth due to a longer growth period and finally a smooth epilayer has grown. A similar epilayer growth process occurred in all orientations; however, the appearance and disappearance of steps depends on growth time.

Lateral growth was observed in all orientations except for [011] and [01-1]. To understand lateral growth in these orientations, the [011] orientated epilayer was cleaved along the [01-1] orientation and the [01-1] orientated epilayer was cleaved along the [011] orientation. The cross-section images of [011] and [01-1] orientated epilayers of 3 and 6 h growth are shown in Fig. 3 (a)-(d). In the [011] orientation, the epilayer growth rate was higher at window walls compared to its centre, termed edge growth, as shown in Fig 3(a). The vertical growth of the epilayer at the walls created the {100} facet at the top, which caused the sluggishness in vertical growth. On the other hand, growth was promoted towards the centre from the wall and finally the thickness discrepancy along the window was removed, as shown in Fig. 3 (b) after 6 h growth. Since two {111} facets are formed at each side face, lateral growth was suppressed. Similarly, {111} facets are formed at side faces in the [01-1] orientation; as a result, limited growth was observed in the lateral direction. Initially, epilayer growth was restricted within the seed window and proceeded in a vertical direction like a trapezoid structure. The fast growing {100} front increased the length of the slow-growing side front {111} with respect to time; as a result, a trapezoid epilayer was formed.

3.2 Star pattern growth by CCLPE

Fig.4 (a)-(d) shows the GaAs layers grown on GaAs substrate with the seed orientations [011], [012], [010], [01-2] and [01-1] by CCLPE with 5 Acm^{-2} current density. The growth

period was (a) 0.5 h, (b) 2 h, (c) 3 h and (d) 6 h, respectively. Since the epilayers grown are conducting in nature, current passes through the epitaxial layer. Therefore, when current is introduced during growth, it brings more solute atoms to the seed window by electromigration, which enhances supersaturation at the interface. Therefore, solute is effectively used for epitaxial growth and lateral and vertical growth was enhanced in all orientations. This was clearly evident when comparing LPE growth and CCLPE growth after 6 h (Fig 2(d) vs 4(d)).

Figure 5 shows the lateral thickness of GaAs epilayer grown for 6 h on the seed windows of different orientations with respect to the applied current. The current density was varied up to 7.5 Acm^{-2}. To maintain measurement consistency and accurate evaluation, lateral growth thickness was measured in all orientations at a distance of 2.5 mm from the centre of the epilayer. The white dotted line in Fig. 4 (d) shows the position of lateral growth measurement. When a current was not applied, lateral growth was very limited in [011] and [01-1] seed orientations. However, it was enhanced in [012], [010] and [01-2] orientations. The largest lateral thickness was 156 μm in the [012] orientation. Even if the current density was increased to 2.5Acm^{-2}, there was no significant improvement of lateral growth. This suggests that the magnitude of driving force, i.e. electromigration by this current density, was not sufficient to bring more solute atoms to the seed window. When the applied current density was increased to 5 Acm^{-2}, lateral growth thickness in [011] and [01-1] seed orientations increased 4- and 3-fold compared to the layer grown under zero current density, respectively. It increased further to 11- and 5-fold at 7.5 Acm^{-2} current density. In [012] and [01-2] seed orientations, lateral growth increased 1.75- and 1.5-fold at 5 Acm^{-2} and 2-fold at 7.5 Acm^{-2} in these orientations. At the [010] seed orientation, lateral growth was gradually increased with respect to current density and it increased by 50% at 7.5 Acm^{-2}. At zero current density, solute transport was mainly due to diffusion. When a current

was applied, electromigration became a main factor for solute transport. Initially, the electric current could only flow through the seed window since the mask layer is an insulating film. When the grown layer exceeded the mask thickness, the surface area of the epitaxial layer was increased by the formation of side faces. Since the layer is conducting in nature, the electric current distribution in the solution was altered by the side faces. Since solute transport due to electromigration was enhanced, growth on the side faces was increased. When the applied current density was increased, the magnitude of solute attraction by the side faces was increased, bringing about an increment of lateral growth in all orientations.

The epilayers were cleaved along their cross-sections and the vertical thicknesses were analyzed by SEM. Fig. 6 shows the vertical thickness of an epilayer with respect to applied current density at different orientations. The vertical thickness was increased proportionally in all orientations by increasing the applied current density. The electric current brought more solute atoms to the growth interface irrespective of orientation by electromigration, which led to an increase in epilayer thickness. The dependence of vertical thickness on seed orientation was also evident. At 7.5 Acm^{-2}, the vertical thickness was 268, 260, 240, 240 and 200 μm in the [01-1], [01-2], [011], [010] and [012] orientations, respectively. The highest vertical thickness was attained in the [01-1] orientation. In the [01-1] orientation, since the {111} facet was formed at the side walls, lateral growth was suppressed. Therefore, the solute was consumed for vertical growth. On the other hand, the lowest vertical thickness was attained in the [012] orientation because the solute atoms were effectively used for lateral growth. The [01-2] orientation has higher lateral and vertical growth.

Peltier cooling occurs at the interface while current flows from substrate to solution, therefore knowledge of Peltier cooling at the interface is an important parameter to understand

the epitaxial growth process in CCLPE. The steady state heat transfer analysis proposed by Stefanakos et al was followed to calculate Peltier cooling at the interface [32]. Considering the electrical analog circuit of growth system geometry as shown in Fig 7 (a), the temperature difference (ΔT) between the GaAs substrate and Ga-rich GaAs solution is given by

$$\left(T_1 - T_0\right) = \frac{-2\pi J}{G_1 + 4G_2 + G_3} \tag{1}$$

where $G_1 = K_{Ga}A/L_1$, $G_2 = K_{GaAs}A/d$ and $G_3 = K_{GaAl}A/L_2$ are thermal conductance of gallium solution, GaAs substrate and GaAl contact solution, respectively. K_{Ga}, K_{GaAs} and K_{GaAl} are thermal conductivities of Ga solution, GaAs and GaAl solution. A, L_1, L_2, d, π, J are area, length of growth solution, length of contact solution, thickness of substrate, Peltier coefficient of GaAs and applied current density, respectively. (T_1-T_0) is proportional to the applied current density through the sample. In table 1, data used in the calculation of Peltier cooling at the interface is presented.

Fig. 7 (b) presents the dependence of temperature change (ΔT) due to Peltier cooling at the substrate-solution interface on applied current density calculated on the basis of equation (1). It indicates that the calculated value of 0.24ºC at 10 Acm^{-2} at 800°C is in good agreement with the experimentally measured value by 0.28ºC [33]. Peltier cooling at the growth interface is responsible for supersaturating the solution for epitaxial growth. The combined effect of Peltier cooling, standard furnace cooling and electromigration contributes to epitaxial growth in CCLPE. However, the observed thickness was much higher than that in standard LPE condition. Since the temperature drop at the interface due to Peltier cooling at 7.5 Acm^{-2} is 0.18°C but is much lower than the change in interface temperature by furnace cooling of 0.6°C/min. This indicates that electromigration is the dominant factor enhancing the growth thickness in all orientations.

The epilayer grown on the [012] seed orientation by CCLPE was used for EPD analysis since it has high lateral growth. The EPD patterns of GaAs (100) substrate and epilayer are shown in Fig. 8 (a) and (b), respectively. The substrate has an average EPD of 10^6 cm^{-2}. The dashed lines in Fig 8 (b) indicate the seed window and dotted lines indicate the EPD measurement points. EPD was measured with an interval of 100 μm between A-A^1 and B-B^1. Fig. 8 (c) shows the EPD profiles along the cross-section of A-A^1 and B-B^1. The EPD of the epilayer grown on a seed window is between 10^5 to 10^6 cm^{-2} and a laterally grown epilayer is 5 x 10^3 cm^{-2}. The defects could be effectively reduced in a laterally grown epilayer by the CCLPE method.

4. Conclusions

Selective epitaxial growth of GaAs on different seed orientations by LPE and CCLPE has been investigated. Vertical and lateral growths were greatly improved in all orientations by CCLPE growth. The highest vertical growth thickness of 260 μm in the [01-2] orientation and the largest lateral growth thickness of 318 μm in the [012] orientation was achieved at a relatively low growth period of 6 h by CCLPE with a current density of 7.5 Acm^{-2}. The electromigration of solute species to the growth interface is the dominant driving force for increased thickness in all orientations. Seed aligned in the [012] orientation are favorable for high lateral growth of GaAs. The seed orientations [011], [010] and [01-2] are suitable for application of GaAs to medical imaging X-ray detectors. CCLPE proved to be a good method to grow a thick GaAs epilayer laterally as well as vertically within a relatively low growth period.

Figure caption

Fig. 1 Schematic diagram of the patterned substrate and its orientation.

Fig. 2 Surface morphologies of GaAs epilayers grown by LPE as a function of time
(a) 0.5 h, (b) 2 h, (c) 3 h, (d) 6 h.

Fig. 3 Cross-sectional images of the [011] orientation (a) 3 h, (b) 6 h, growth and the [01$\bar{1}$]
orientation (c) 3 h, (d) 6 h growth.

Fig. 4 Surface morphologies of GaAs epilayers grown by CCLPE with 5Acm^{-2} current density
as a function of time (a) 0.5 h, (b) 2 h, (c) 3 h, (d) 6 h.

Fig. 5 Lateral thickness of GaAs epilayer with respect to seed orientation as a function of
current density for 6 h growth.

Fig. 6 Vertical thickness of GaAs epilayer with respect to current density on different seed
orientations for 6 h growth.

Fig. 7 (a) Schematic diagram of electrical analog circuit of growth solution-substrate-contact
solution, (b) Calculated ΔT by Peltier cooling at the substrate-solution interface.

Fig. 8 Optical photograph of KOH etched (a) GaAs substrate (b) GaAs epilayer grown on the
[012] orientation with current density of 5Acm^{-2} for 6 h and (c) EDP profiles along the cross-
section of laterally grown epilayer.

References

[1] M.J. Yaffe, J.A Rowlands, Phys. Med. Biol. **42** (1997) 1.

[2] L.B. Schein, Phys. Rev. B **10** (1974) 3451.

[3] M.L. Benkhedir, M. Brinza, N. Qamhieh, G.J. Adriaenssens, J. Non-Cryst. Solids **352** (2006) 1543.

[4] M. Zahangir Kabir, M. Yunus, S.O. Kasap, O. Tousignant, H. Mani, P. Gauthier, Currt. Appl. Phys **6** (2006) 393.

[5] G.C. Sun, H. Samic, J.C. Bourgoin, D. Chambellan, O. Gal, Ph. Pillot, IEEE Trans. Nucl. Sci. **51** (2004) 2400.

[6] J.C. Bourgoin, Nucl. Instrum. Methods A **460** (2001) 159.

[7] G.C. Sun, N. Talbi, C. Verdeil, J.C. Bourgoin, Appl. Phys. Lett. **85** (2004) 2399.

[8] A.V. Markov, A.Y. Polyakov, N.B. Smirnov, A.V. Govorkov, V.I. Biberin, N.S. Korovin, et al. Solid State Electron **46** (2002) 2161.

[9] A.V. Markov, V.I. Biberin, A.Y. Polyakov, N.B. Smirnov, A.V. Govorkov, V.N. Gavrin, et al. Solid State Electron **51** (2007) 1039.

[10] D.F. Bliss, C. Lynch, D. Weyburne, K. Ohearn, J.S. Bailey, J. Cryst. Growth **287** (2006) 673.

[11] C. Lynch, D.F. Bliss, T. Zens, A. Lin, J.S. Harris, P.S. Kuo, M.M. Fejer, J. Cryst. Growth **310** (2008) 5241.

[12] T. Bryskiewicz, M. Bugajski, J. Lagowski, H. C. Gatos, J. Cryst. Growth **87** (1982) 36.

[13] H. Sheibani, S. Dost, S. Sakai, B. Lent, J. Cryst. Growth **258** (2003) 283.

[14] S. Naritsuka, Y. Tejima, K. Fujie, T. Maruyama, J. Cryst. Growth **310** (2008) 1642.

[15] S. Saki, Y. Ohashi, Y. Shintani, J. Appl. Phys. **70** (1991) 4899.

[16] S. Sakawa, T. Nishinaga, Jpn. J. Appl. Phys. **31** (1992) L359.

[17] S. Naritsuka, T. Nishinaga, J. Cryst. Growth **146** (1995) 314.

[18] Y.S. Chang, S. Naritsuka, T. Nishinaga, J. Cryst. Growth **174** (1997) 630.

[19] S. Naritsuka, T. Nishinaga, J. Cryst. Growth **222** (2001) 14.

[20] Y. Hayakawa, K. Balakrishnan, S. Iida, Y. Shibata, T. Koyama, M. Kumagawa, J. Cryst. Growth **229** (2001) 158.

[21] M.G. Mauk, J.P. Curran, J. Cryst. Growth **225** (2001) 348.

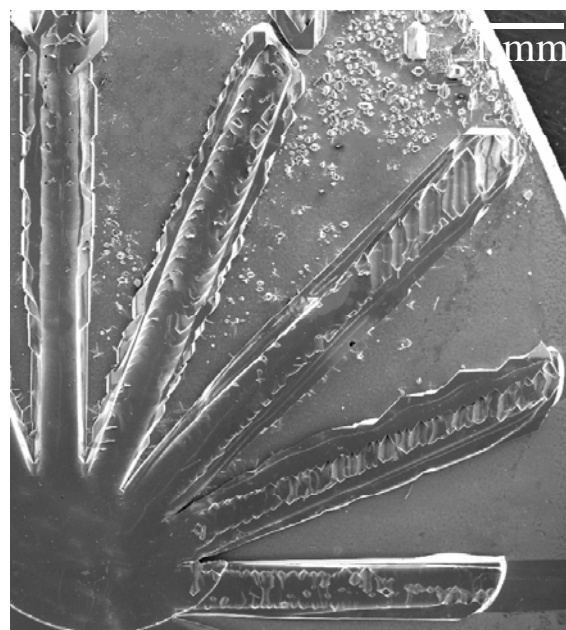[22] K. Balakrishnan, S. Iida, M. Kumagawa, Y. Hayakawa, Semicond. Sci. Technol., **17** (2002)

729.

[23] G. Zhang, K. Balakrishnan, T. Koyama, M. Kumagawa, Y. Hayakawa, J. Cryst. Growth **256** (2003) 243.

[24] D. Dobosz, Z. R. Zytkiewicz, E. Papis, E. Kaminska, A. Piotrowska, J. Cryst. Growth **253** (2003) 102.

[25] G. Zhang, K. Balakrishnan, T. Koyama, M. Kumagawa, Y. Hayakawa, J. Cryst. Growth **275** (2005) e931.

[26] Z.R. Zytkiewicz, D. Dobosz, Y.C. Liu, S. Dost, Cryst. Res. Technol. **40** (2005) 321.

[27] Y.S. Chang, S. Naritsuka, T. Nishinaga, J. Cryst. Growth **312** (2010) 629.

[28] T. Nishinaga, T. Nakano, S. Zhang, Jap. J. Appl. Phys. **27** (1988) L964.

[29] Z. Zhang, T. Nishinaga, J. Cryst. Growth **99** (1990) 292.

[30] S. Sakawa, T. Nishinaga, J. Cryst. Growth **115** (1991) 145.

[31] D. Mouleeswaran, T. Koyama, Y. Hayakawa, J. Cryst. Growth **311** (2009) 3314.

[32] L. Jastrzebski, L. Lagowski, H.C. Gatos, A.F. Witt, J. Appl. Phys. **49** (1978) 5909.

[33] E.K. Stefanakos, A. Abul-Faadl, M.D. Workman, J. Appl. Phys. **46** (1975) 3002.

Fig. 1.

Fig. 2.

(a)

(b)

(c)

(d)

Fig. 3.

Growth time (h)	[011] orientation	[01-1] orientation
3	(a)	(c)
6	(b)	(d)

Fig. 4.

(a)

(b)

[011]
[012]
[010]
[01$\bar{2}$]
[01$\bar{1}$]

(c)

(d)

{111}
{111}

Fig. 5.

Fig. 6.

Fig. 7

Ga-rich GaAs solution

GaAs Substrate

Ga+Al Contact solution

G_1

G_2

G_3

$-\pi J$

$+\pi J$

T_0

T_1

T_2

$-$

$+$ T_0

(a)

ΔT at the interface $(T_1 - T_0)$ °C

Current density (J)

(b)

Fig. 8

(a)
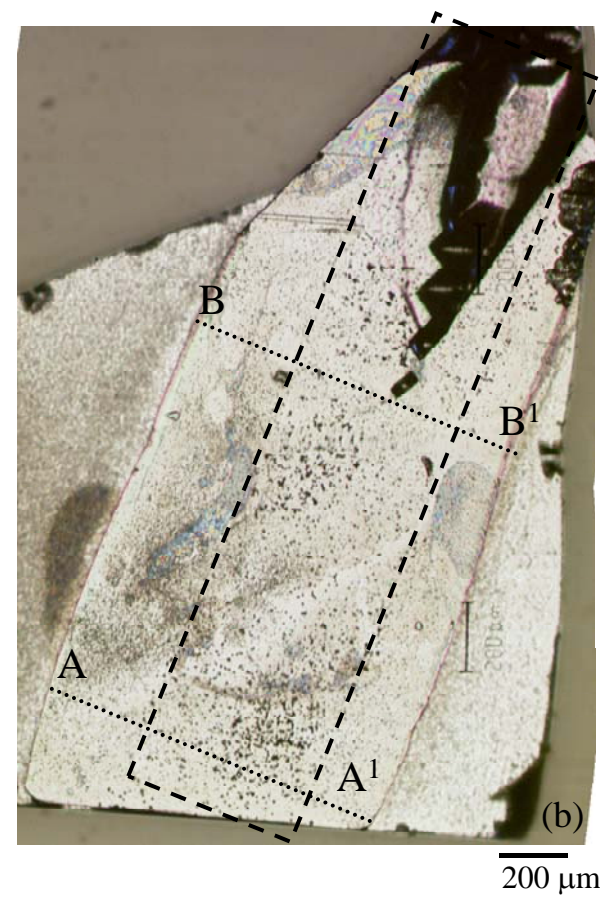
10 µm
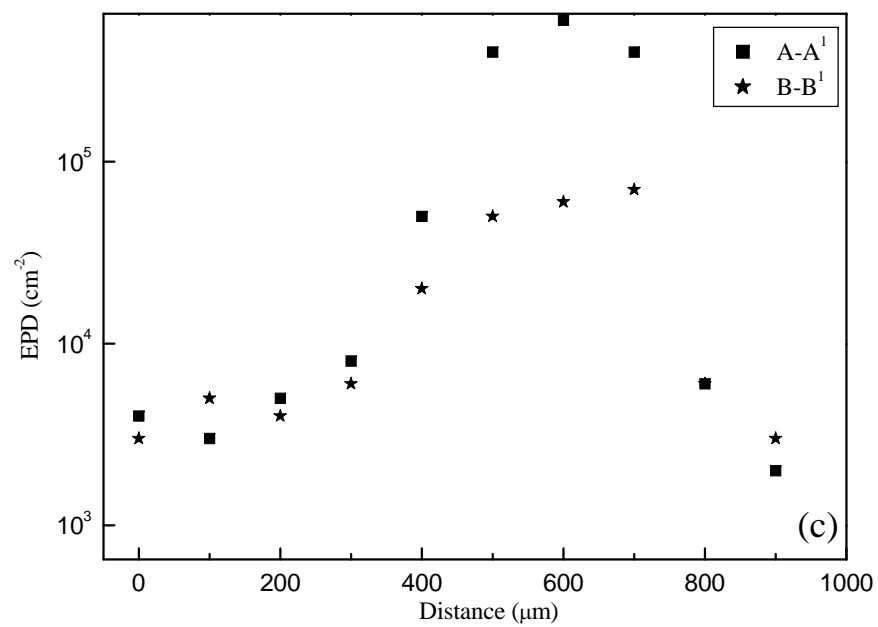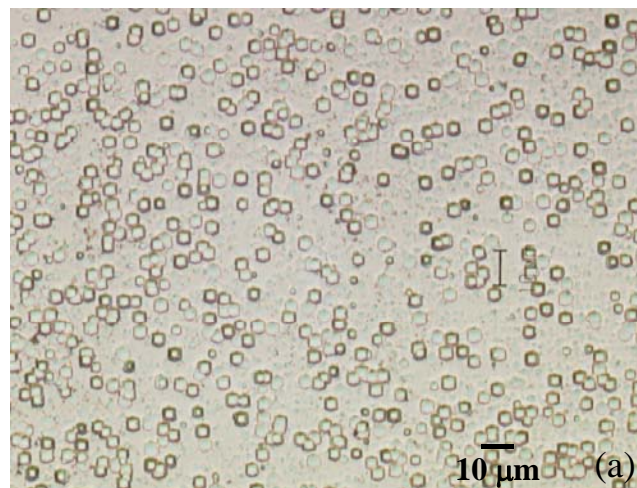
(b)

200 µm

(c)
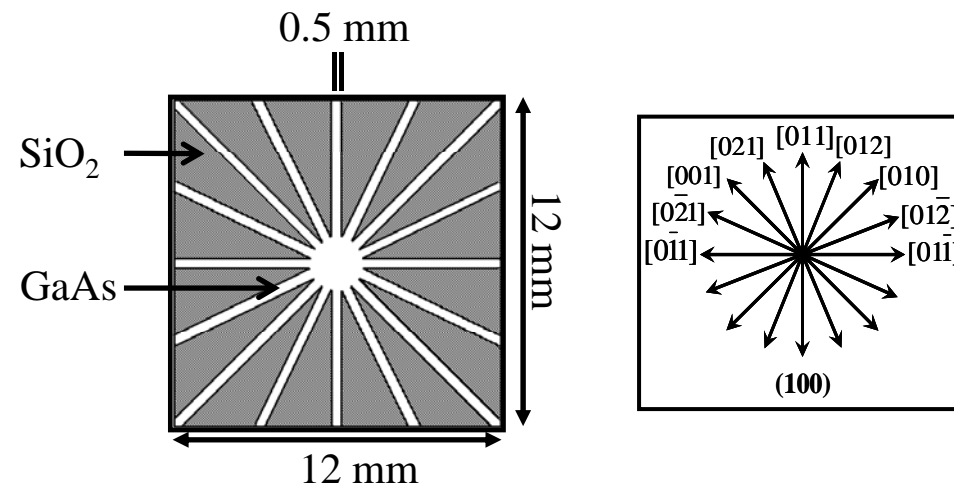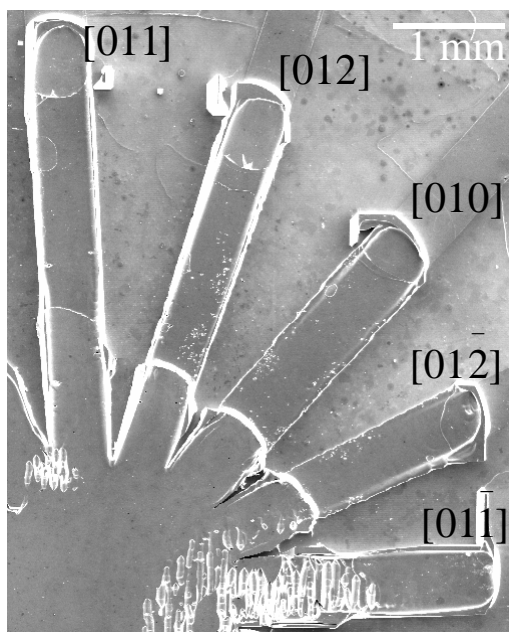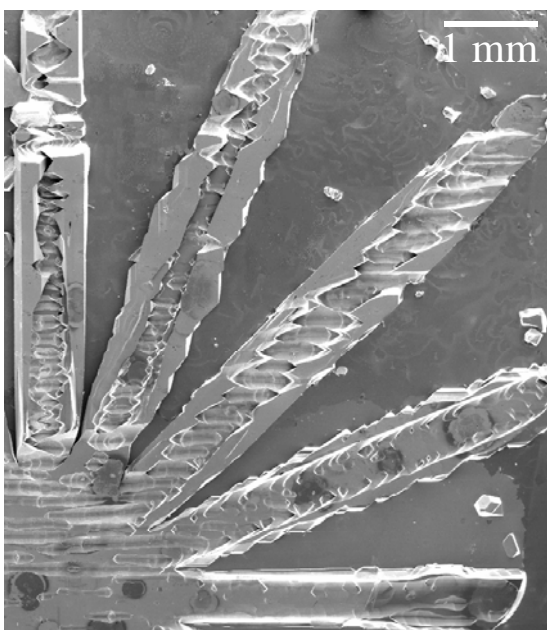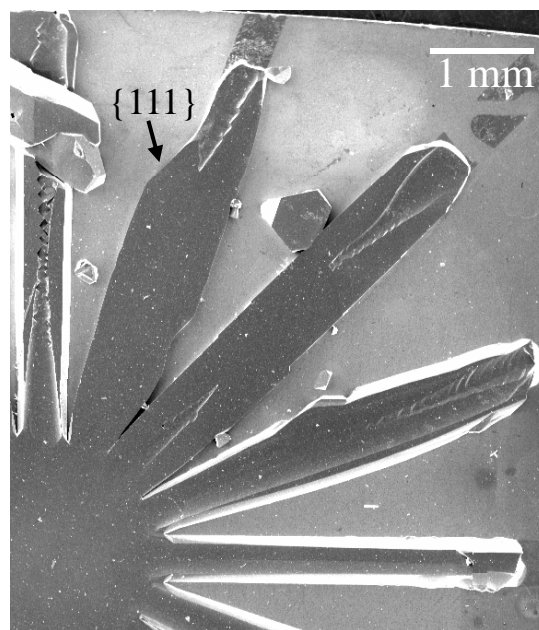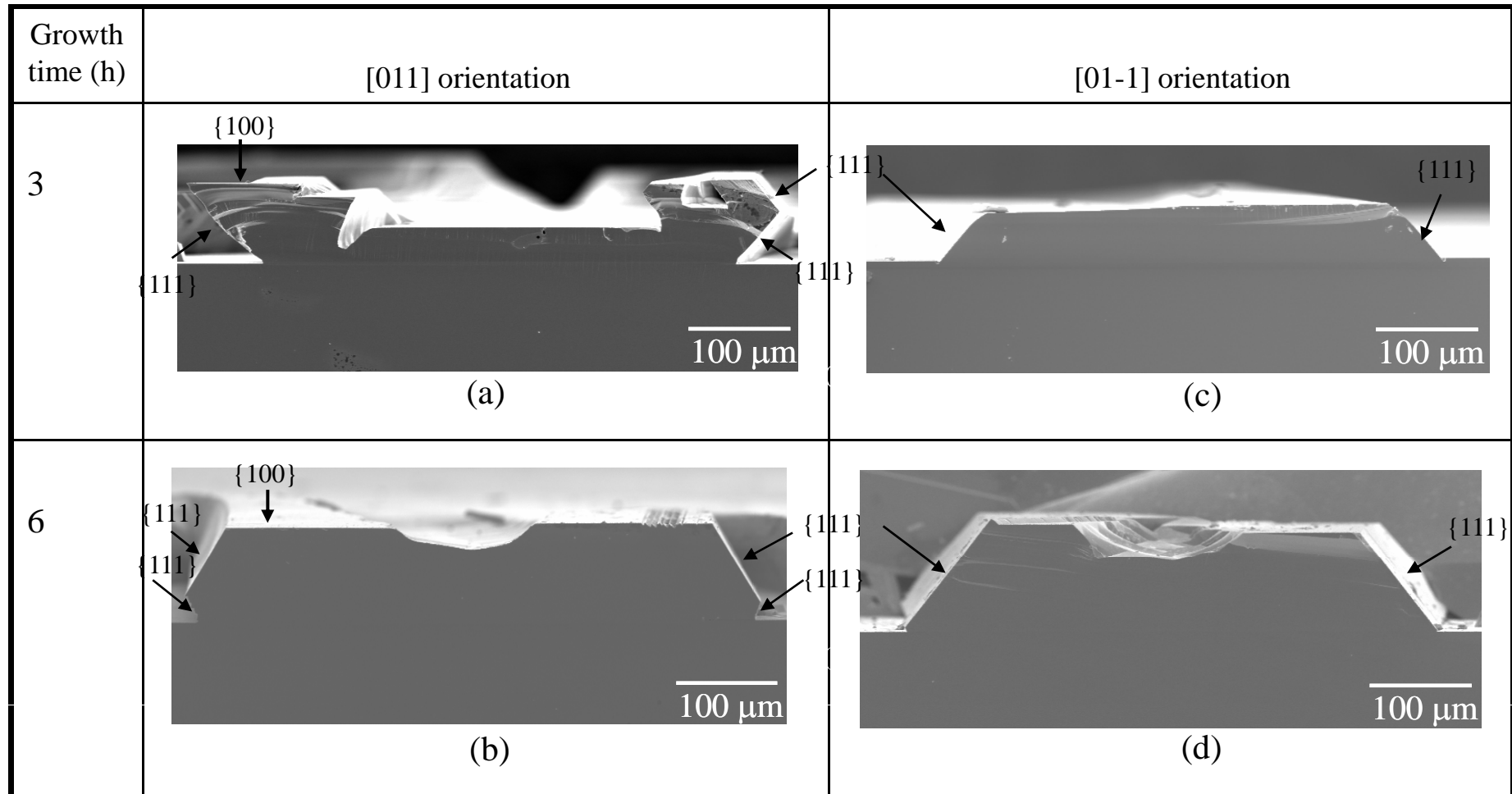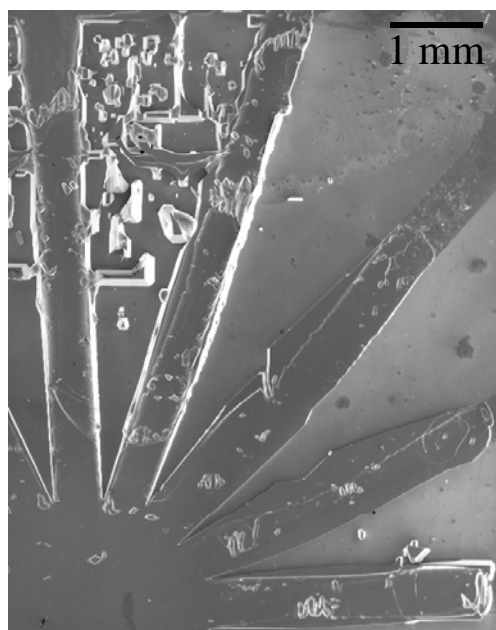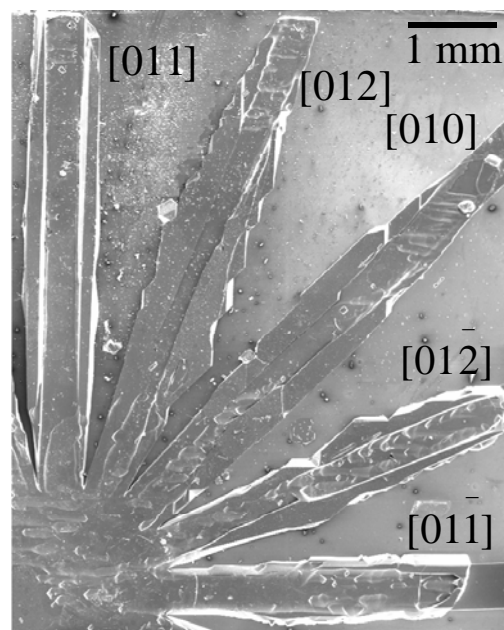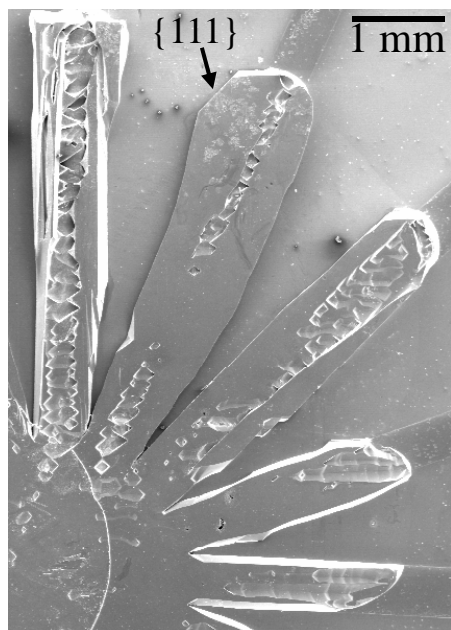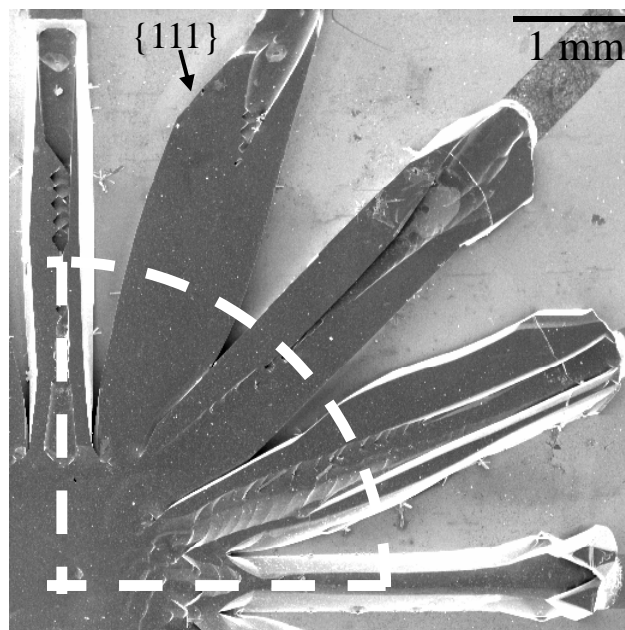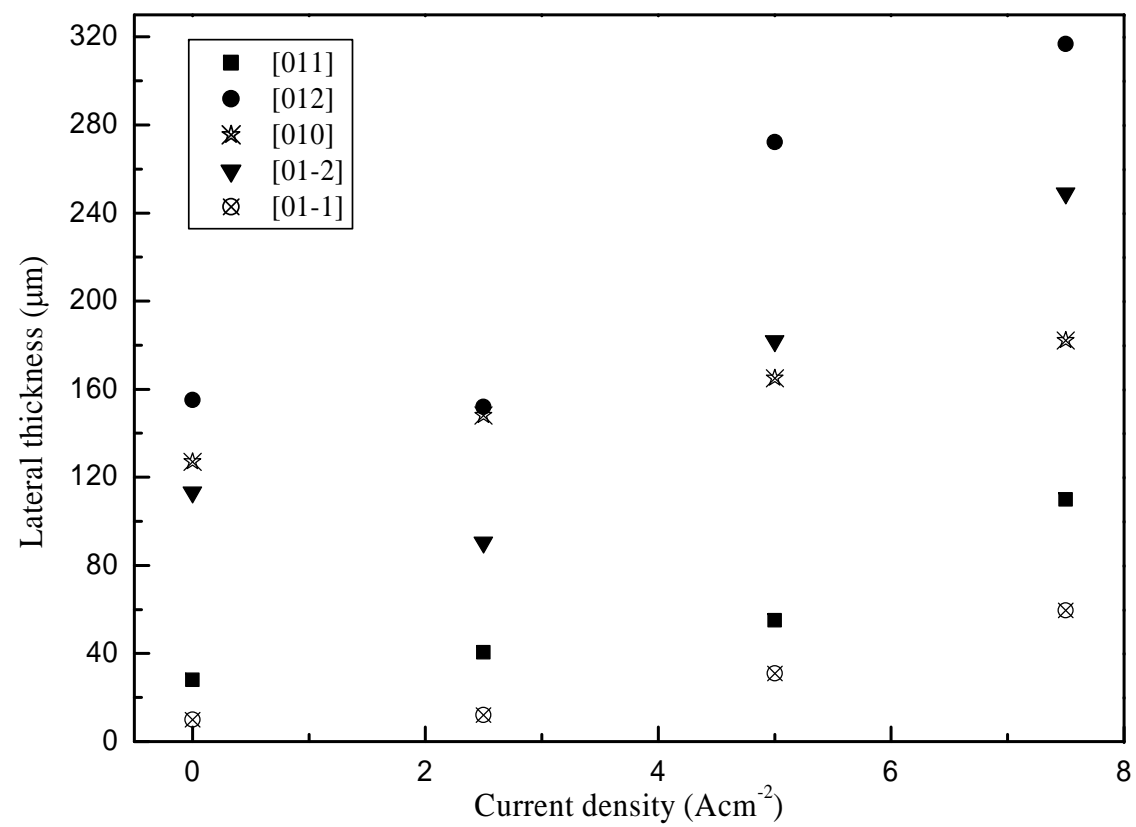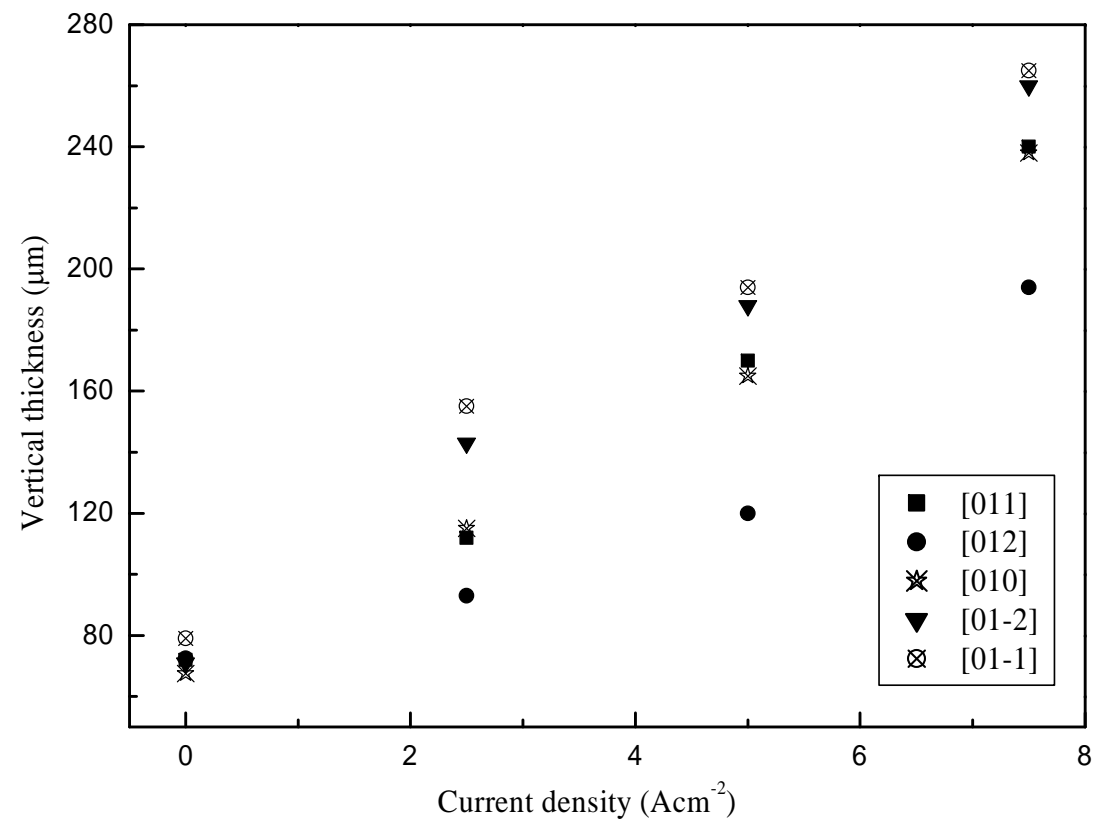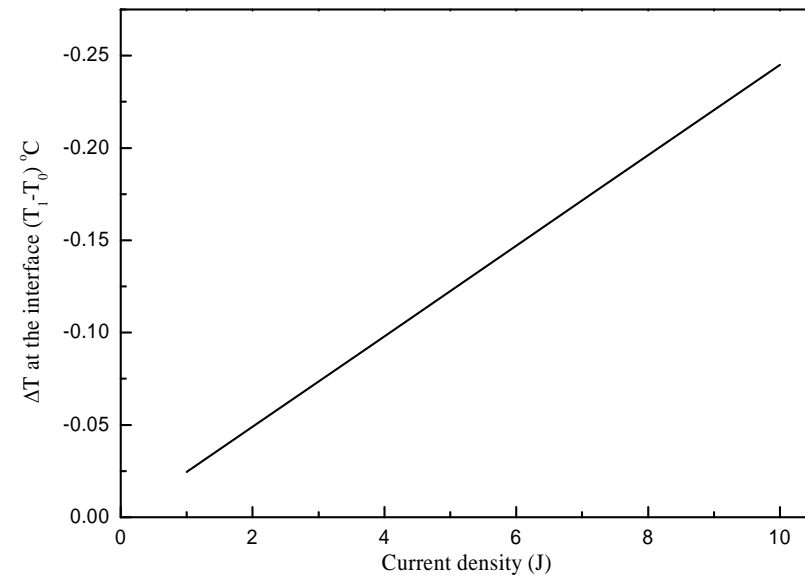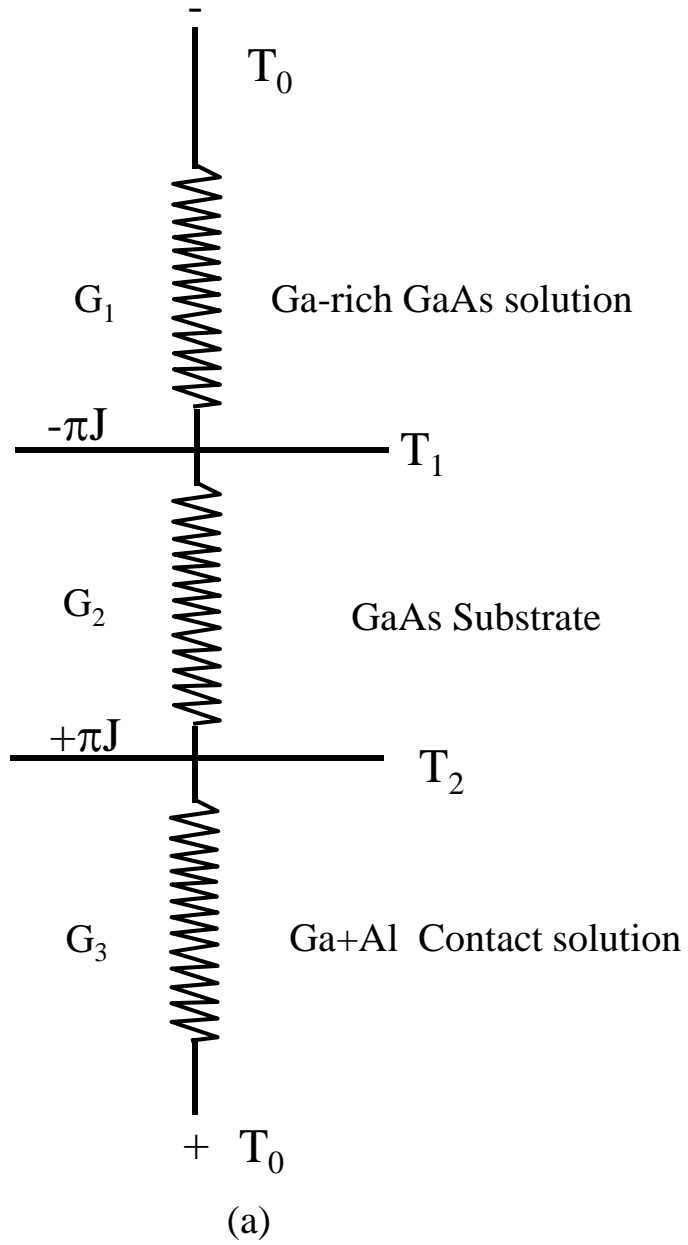
Table: 1

Parameters	
Temperature	800°C
Thermal conductivity of gallium solution K_{Ga}	0.526 W/cm °C
Thermal conductivity of GaAs substrate K_{GaAs}	0.082 W/cm °C
Thermal conductivity of gallium aluminum solution K_{GaAl}	0.738 W/cm °C
Peltier coefficient of GaAs π	0.2 V
Length of gallium solution L_1	0.7 cm
Length of gallium aluminum solution L_2	0.2 cm
Thickness of substrate d	0.035 cm